Published in final edited form as:
J Infect Dis. 2010 October 1; 202(7): 1136–1145. doi:10.1086/656191.

Metallomic Analysis of Macrophages Infected with *Histoplasma capsulatum* Reveals a Fundamental Role for Zn in Host Defenses

Michael S. Winters[1], **Qilin Chan**[2], **Joseph A. Caruso**[2], and **George S. Deepe**[1,3]

[1] Division of Infectious Diseases, University of Cincinnati College of Medicine, Cincinnati, OH 45267, USA

[2] Department of Chemistry, University of Cincinnati, Cincinnati, OH 45221-0172, USA

[3] Veterans Affairs Hospital, Cincinnati, OH 45220, USA

Abstract

The fungal pathogen *Histoplasma capsulatum* evades the innate and adaptive immune responses and thrives within resting macrophages (Mφ). Cytokines that induce antimicrobial activity such as granulocyte macrophage-colony stimulating factor (GM-CSF) inhibit *H. capsulatum* growth in Mφ. Conversely, interleukin 4 (IL-4) inhibits the killing of intracellular pathogens. Using inductively coupled plasma mass spectrometry, we examined alterations in metal homeostasis of murine *H. capsulatum*-infected Mφ infected that were exposed to activating cytokines. Restriction of iron ($Fe^{2+/3+}$) and zinc (Zn^{2+}) was observed in infected, GM-CSF-treated Mφ compared to infected controls. IL-4 reversed the anti-fungal activity of GM-CSF-activated Mφ and was associated with increased intracellular Zn^{2+}. Chelation of Zn^{2+} inhibited yeast replication both in the absence and presence of Mφ. Treatment of cells with GM-CSF altered the host Zn^{2+} binding species profile. These results establish that Zn^{2+} deprivation may be a host defense mechanism utilized by Mφ.

Keywords

Histoplasma capsulatum; macrophages; mass spectrometry; zinc; cytokines

Introduction

H. capsulatum infection is initiated by inhalation of fungal spores followed by conversion to the pathogenic yeast phase. Infection is controlled in most immunocompetent individuals but establishes a persistent state. Histoplasmosis can be life-threatening for individuals suffering from immune defects arising from HIV infection or receiving drugs for malignancy, graft rejection, or au-toimmune diseases. More recently, tumor necrosis factor (TNF)-α antagonists have been linked to higher incidence of histoplasmosis [1].

Alveolar macrophages (Mφ) are the presumed first line of cellular defense *H. capsulatum* encounters in the host. Mφ are the only professional phagocytic cell population in which *H. capsula-tum* replicates freely [2], although growth is inhibited following cytokine activation of Mφ. Interfe-ron gamma (IFN)-γ and granulocyte macrophage-colony stimulating factor

Reprints or correspondence: Michael S. Winters, Division of Infectious Diseases, Department of Medicine, University of Cincinnati College of Medicine, Cincinnati, Ohio 45267-0560. Phone-513-558-4704; fax-513-558-2089; winterms@ucmail.uc.edu.

The authors report no conflicts.

This manuscript was not presented at a meeting.

(GM-CSF) restrict growth in mouse and human Mφ respectively [3,4]. One mechanism by which IFN-γ inhibits *H. capsulatum* intracellular growth is by restricting iron ($Fe^{2+/3+}$) [3]. Much of this data has been accrued by adding exogenous Fe to cells or restricting access to $Fe^{2+/3+}$. A missing analysis has been a direct measurement of Fe or any metal present within phagocytes or pathogens harbored by these cells.

Since metals are critical to the functional integrity of cells, we sought to determine if there was a correlation between metal uptake of *H. capsulatum* infected Mφ activated by cytokines. We observed that Zn^{2+} and $Fe^{2+/3+}$ levels were restricted inside GM-CSF-treated Mφ infected with *H. capsulatum* compared to resting Mφ. Zn^{2+} binding species were differentially regulated within resting Mφ versus GM-CSF-treated cells. Chelating Zn^{2+} reduced *H. capsulatum* growth in medium and within resting Mφ. Moreover, pretreating GM-CSF-activated Mφ with IL-4 reversed growth inhibition, and partially replenished Zn^{2+} levels. These data support an important role for Zn^{2+} restriction as a host defense strategy to *H. capsulatum* infection.

Methods

Mice

Six to eight week old C57BL/6 mice were purchased from Jackson Laboratories, Bar Harbor, Maine. Animals were housed in isolator cages and maintained by the Department of Laboratory Animal Medicine, University of Cincinnati, which is accredited by the Association for Assessment and Accreditation of Laboratory Animal Care. All animal experiments were performed in accordance with the Animal Welfare Act guidelines of the National Institutes of Health. All protocols were approved by the University of Cincinnati Institutional Animal Care and Use Committee.

Reagents

Sodium dodecyl sulfate (SDS), high performance liquid chromatography (HPLC)-grade water, methanol, diethylenetriaminepenta-acetic acid (DTPA), ethylene glycol tetraacetic acid (EGTA), N,N,N′,N′-Tetrakis-(2-pyridylmethyl) ethylenediamine (TPEN), $ZnSO_4$, $FeSO_4$, and F-12 Ham's were purchased from Sigma Aldrich (St. Louis, MO). Recombinant mouse GM-CSF, IFN-γ, and IL-4 were acquired from PeproTech (Rocky Hill, NJ). Arginase, YM1, and FIZZ1 primers for RT-PCR analysis were purchased from Applied Biosystems (Foster City, CA) and TRIzol was purchased from Invitrogen (Carlsbad, CA). Diff-Quik stain kit was obtained from IMEB Inc. (San Marcos, CA).

All solutions for ICPMS analysis were prepared in 18 MΩ cm^{-1} double deionized water (Sybron Barnstead, Boston, MA), in which no metal was detected. The mobile phase for size-exclusion chromatography (SEC) was made by dissolving tris(hydroxymethyl)aminomethane (Tris) in double deionized water and adjusting the pH with hydrochloric acid. The SEC standard (Bio-Rad Laboratories, Inc., Hercules, CA) is a lyophilized mixture of molecular weight markers ranging from 1,300 to 670,000 Da.

H. capsulatum intracellular growth assays

Murine alveolar (A) Mφ, bone marrow derived (BM) Mφ, and peritoneal (P) Mφ were used. AMφ were prepared by consecutive lung lavages, rinsing 5x with 1 ml of phosphate buffered saline (PBS). PMφ were acquired by lavaging peritoneal cavities with 10 ml of PBS. BMMφ were generated by extracting bone marrow cells from the femurs of mice, and cells were incubated in RPMI-1640 growth media at 37°C in the presence of GM-CSF (10 ng/ml) and 5% CO_2 for 5–6 days. In some experiments, cells were incubated with 10 ng/ml of IL-4 for another 24 hr following 5 day incubation with GM-CSF. PMφ were incubated with 10 ng/ml of either GM-CSF or IFN-γ for 24 hr. All Mφ were plated at 1×10^5 cells/well in a 96-well plate.

H. capsulatum strain G217B yeasts were grown as previously described [5]. Mφ were infected with *H. capsulatum* at a multiplicity of infection of 5X yeasts/Mφ; growth inside Mφ was quantified by plating. Infected Mφ were lysed in sterile water and lysates plated onto Mycosel agar 5 (Becton Dickinson) plates containing 5% sheep blood and 5% glucose. Plates were incubated at 30°C for 1 wk.

The leucine assay was used for metal chelation and supplementation experiments [4]. For metal supplementation experiments $ZnSO_4$ or $FeSO_4$ were added (100 μM) to media (RPMI-1640), and for metal chelation experiments TPEN or DTPA was added prior to infection. Toxicity of TPEN, DTPA, and $ZnSO_4$ was measured using trypan blue stain.

Sample preparation for ICPMS analysis of infected Mφ and intracellular yeasts

Mφ were plated at 1×10^6 per well in a 12-well plate and infected with *H. capsulatum* at a multiplicity of infection of 5X. After 24 hr, cells were washed with HBSS. Infected Mφ were treated (~1 min) with 250 μl of 0.1% SDS in water per well. Metal concentrations in 0.1% SDS and wash buffer (HBSS) were less than 10 ppb (μg L^{-1}) for all metals except sodium,.

For metal analysis of intracellular *H. capsulatum*, yeasts were isolated from infected Mφ following 0.1% SDS and centrifugation. Each group of intracellular yeasts isolated were set at 1×10^8/10 μl using a hemacytometer.

Yeasts and infected Mφ were further diluted 1:1.25 to set at a concentration of 20% HNO_3. Before ICPMS analysis of infected Mφ and isolated organisms, each sample was subjected to microwave digestion using a closed-vessel CEM Discover-Explorer microwave digestion system (CEM Corporation, Matthews, NC, USA). The digestion process was performed at 150 °C for 2 min by maintaining a pressure below 250 psi.

For SEC and ICPMS analysis samples were not subjected to microwave digestion. Infected Mφ were immediately centrifuged following 0.1% SDS treatment, and *H. capsulatum* removed. The supernatant was stored at −70 °C before ICPMS analysis.

ICPMS analysis

ICPMS-based quantification has been commonly used to determine accurate concentration of multiple metals simultaneously in biological samples [6,7]. ICPMS metal analysis was performed on an Agilent 7500ce ICPMS (Agilent Technologies, Santa Clara, CA,). A conventional Meinhard nebulizer, a Peltier-cooled spray chamber (2°C) and a shield torch constitute the sample introduction system under standard plasma conditions.

HPLC was performed using flow injection, and SEC were carried out with an Agilent 1100 liquid chromatograph (Agilent Technologies, Santa Clara, CA, USA) equipped with a binary HPLC pump, an autosampler, a vacuum degasser system, a temperature column compartment and a diode array detector. The outlet of the HPLC/UV detector was connected to a sample inlet of the ICPMS nebulizer using 0.25 mm i.d. polyether ether ketone tubing of 30 cm in length. Both UV (wavelength = 280 nm). ICPMS signals were collected online.

A Superdex 200 10/300 GL column (10 mm × 300 mm, 13 μm) (Amersham Pharmacia Biotech, Uppsala, Sweden) was used for SEC analysis. The column was calibrated with a UV detector (wavelength = 280 nm) using a gel filtration standard mixture (thyroglobulin MW=670 kDa, γglobulin MW=158 kDa, ovalbumin MW=44 kDa, myoglobin MW=17 kDa, vitamin B_{12} MW=1.3kDa), purchased from Bio-Rad Laboratories, Inc. Lysed Mφ (0.1% SDS treated) described above were injected onto the column. ICPMS flow injection analysis and SEC conditions are shown in Table 1.

Intracellular H. capsulatum counting

The number of organisms within each cytokine treated Mφ population following 5X yeasts/Mφ ratio was counted by staining cells with Diff-Quik and counting at least 100 infected Mφ.

Flow cytometry

Two hundred thousand Mφ were treated with IL-4 for 24hr and then exposed to *H. capsulatum*. Cells were then stained with Peridinin Chlorophyll Protein Complex (PerCP) - conjugated CD11b and allophycocyanin (APC)-CD71 (BD Biosciences, San Jose, CA). Cells were then stained with APC-conjugated CD71 antibodies. Flow cytometry analysis was performed on Mφ infected with *H. capsulatum* (5X yeasts/Mφ ratio) expressing green fluorescent protein [8] and PerCP-CD11b to determine the percentage of infected cells. Staining for both groups was done at 4°C for 15 min in HBSS containing 1% BSA and 0.01% sodium azide. Cells were washed and resuspended in 1% paraformaldehyde to fix. Isotype controls were performed in parallel. Fluorescence intensity was assessed using a FACS Caliber (BD Biosciences) and analyzed using FCS Express Software.

Real-time reverse transcriptase polymerase chain reaction (qRT-PCR)

A total of 5×10^5 Mφ were infected with 5X yeasts/Mφ ratio. Following 24hr total RNA from Mφ was isolated using TRIzol. Oligo(dT)-primed cDNA was prepared using the reverse transcriptase system (Pro-mega, Madison, WI). qRT-PCR analysis for was performed using Taq-Man Master Mix and primers; HPRT, Arginase, FIZZ1 (Retna), YM1 (Chi3-L3), and calprotectin (S100). Samples were analyzed on an ABI Prism 7500 (Applied Biosystems). In each experiment, HPRT was used as an internal control. The conditions for amplification were 50°C for 2 min, 95°C for 10 min, followed by 40 cycles of 95°C for 15 sec and 60°C for 1 min.

Nitric oxide detection

Nitric oxide levels in infected Mφ (5X yeasts/Mφ ratio) were measured using the Cayman (Ann Arbor, MI) Nitrate/Nitrite colorimetric assay kit. Experiments were performed in triplicate using 5×10^5 BMMφ per well in a 96-well plate.

Statistical analysis

T-test was used to compare two groups while ANOVA analysis was used to compare multiple groups. Differences with $P<.05$ were considered significant.

Results

Intracellular yeast growth in resting vs. GM-CSF-activated Mφ

We previously reported that GM-CSF enhanced host defenses to *H. capsulatum* [9]. Hence, we sought to determine if it acted upon Mφ. Exposure of several populations of Mφ to GM-CSF inhibited the intracellular growth of *H. capsulatum* (Fig. 1). IL-4 blunts immunity to *H. capsulatum* and is associated with the emergence of alternatively activated Mφ [10]. We asked if pre-treatment of Mφ with IL-4 alters intra-cellular growth in activated Mφ [11]. Exposure of Mφ for 24 hr to IL-4 enhanced yeast growth in BMMφ (Fig. 1).

We examined if IL-4 alternatively activated infected Mφ. We assessed the expression of arginase-1, FIZZ1, and YM1 [12]. Each gene manifested enhanced expression following exposure of BMMφ cells to IL-4 and infection with *H. capsulatum* (Fig. 2). The abundance of another marker of IL-4 activation, transferrin receptor (TfR), was analyzed by flow cytometry. IL-4 treatment of Mφ 24 hr before *H. capsulatum* infection did not increase total TfR expression as determined by the mean fluorescent intensity (MFI). The MFI of Mφ exposed to medium (926.6) did not differ from that of cells exposed to 10ng/ml of IL-4 (952.3). Moreover, no

differences in the percentage of cells expressing TfR were observed between the two groups (data not shown). IL-4 did enhance TfR expression on uninfected cells in a dose dependent manner. The MFI of cells exposed to medium only (2055.2) was less than that of cells exposed to 0.1 ng/ml of IL-4 (3763.4), 1 ng/ml (4378.7) or 10 ng/ml (4333.9). Likewise there was an increase in the percentage of cells expressing TfR; 79.5% of cells incubated in medium only were TfR^+ whereas those values were 81.5%, 86.1%, 88.1% for 0.1 ng/ml, 1 ng/ml, and 10 ng/ml of IL-4 respectively.

We did not detect a significant difference in nitric oxide (NO) production between IL-4 treated (5.3 ± .2 μM nitrite) versus untreated Mφ (5.7 ± .4 μM nitrite).

GM-CSF regulates Mφ metal levels

We queried if GM-CSF altered metal levels in cells. We undertook an unbiased approach using ICPMS to assess levels of Mg^{2+}, Ca^{2+}, $Fe^{2+/3+}$, Zn^{2+}, Cu^{2+}, and Mn^{2+} during infection of Mφ.

We determined metal levels in uninfected and infected PMφ and in those pre-treated with [4]. Total metal concentrations were highest in resting uninfected PMφ compared to all other populations (Table 2). We observed decreases in the overall concentrations of metals upon infection, but this restriction was enhanced for $Fe^{2+/3+}$ and Zn^{2+} by GM-CSF activation (Table 2). GM-CSF did induce a decrease in Zn^{2+} in uninfected PMφ, but this was not statistically significant (Table 2).

Mφ from various organs may not regulate metals similarly; hence, Zn^{2+} concentrations in BMMφ and AMφ were measured. Similar to infected PMφ exposed to GM-CSF, infected BMMφ grown in the presence of GM-CSF yielded lower Zn^{2+} and $Fe^{2+/3+}$ levels compared to that of infected resting PMφ (Table 2). A Zn^{2+} concentration of 246 ppb (RSD = 3%, n = 3) was measured in resting AMφ while in GM-CSF treated AMφ was124 ppb (RSD = 6%, n = 3). $Fe^{2+/3+}$ levels were 1200 ppb (RSD = 1.9%, n = 3) in resting AMφ while in GM-CSF treated AMφ levels were 540 ppb (RSD = 4%, n = 3).

To ensure that altered metal levels observed in this study were not a result of different numbers of yeast initially ingested by the Mφ, we counted the number of yeasts within each cytokine treated Mφ population. We observed that following infection of Mφ for 1 hr, each Mφ population contained a mean (± SEM) of 12 ± 3 yeasts. Moreover, utilizing *H. capsulatum* expressing green fluorescent protein, we found that that ~90% of Mφ were infected after 24 hr.

We questioned whether our overall for cellular metal concentrations were acceptable. The cytosolic pool of free Zn in a cell is estimated to range from 10^{-5}-10^{-12} M; our measurements were in the 10^{-7} M range [13,14].

Metal levels within intracellular yeast cells

Total Mφ metal analysis may not dictate the amount within ingested yeasts. Thus, we analyzed metal concentrations of K^+, Mg^{2+}, Ca^{2+}, $Fe^{2+/3+}$, Zn^{2+}, Cu^{2+}, Mn^{2+} and Ni^{2+} within *H. capsulatum* isolated from Mφ. Lower amounts of Zn^{2+} and Ca^{2+} ($P < .05$) were detected in yeasts isolated from BMMφ and GM-CSF-exposed PMφ compared to resting PMφ or *H. capsulatum* grown in culture alone (Table 2).

To validate our methodology, we assessed if IFN-γ pretreatment of PMφ decreased $Fe^{2+/3+}$ levels. A $Fe^{2+/3+}$ concentration with a mean of 2440 ppb (RSD = 7%, n = 3) was detected for *H. capsulatum* isolated from IFN-γ pretreated PMφ compared to resting PMφ mean of 6240 ppb (RSD = 4%, n = 3). Thus, these data support the utility of this method for assaying

intracellular metals. IFN-γ also decreased Zn^{2+} levels. Cytokine treated cells contained 600 ppb (RSD = 6%, n = 3) and resting cells had 1900 ppb, (RSD = 6%, n = 3).

Increases in Zn levels in IL-4 treated Mφ and intracellular yeast cells

We asked if IL-4 enhancement of fungal growth was associated with a change in intracellular metal abundance. Zn^{2+} levels increased >2X inside infected BMMφ treated with IL-4 while $Fe^{2+/3+}$ concentrations did not (Table 2). In addition, higher Zn^{2+} and Ca^{2+} levels were detected in *H. capsulatum* isolated from IL-4 pretreated BMMφ compared to that of untreated cells (Table 2).

Zn influences yeast growth

A decrease of Zn^{2+} levels in activated Mφ coupled with an increase following IL-4 treatment led us to hypothesize that restriction of Zn^{2+} is a host defense mechanism against *H. capsulatum*. We sought to determine the effects of the Zn^{2+} chelators DTPA and TPEN on *H. capsulatum* growth.

DTPA inhibited *H. capsulatum* growth in a dose dependent manner in the presence and absence of PMφ (Fig. 3A and 3B). DTPA was not toxic at the concentrations used in this study. TPEN inhibited *H. capsulatum* growth in a dose dependent manner in the presence and absence of PMφ (Fig. 3C). TPEN is toxic to Mφ at low concentrations therefore we could not adequately interpret TPEN's influence on intracellular yeast growth.

Because TPEN and DTPA bind Fe^{2+} [15] we determined if Fe^{2+} chelation by DTPA and TPEN influenced our results. In the presence of DTPA, $FeSO_4$ and $ZnSO_4$ partially rescue *H. capsulatum* growth in culture alone or inside resting peritoneal Mφ. In the presence of TPEN, the addition of $FeSO_4$ partially enhanced *H. capsulatum* growth whereas $ZnSO_4$ completely restored it.

We examined whether Ca^{2+} had an effect on yeast growth inside Mφ because Ca^{2+} levels were diminished in *H. capsulatum* isolated from GM-CSF treated Mφ and increased following IL-4 treatment. Chelation of Ca^{2+} with EGTA did not significantly influence yeast growth in medium or inside PMφ (Fig. 3D).

GM-CSF regulation of Mφ Zn species

Zn^{2+} is a cofactor and required for numerous host processes [16]. We hypothesized that the changes in total Zn^{2+}would need to be tightly regulated. Thus, we should detect a change in the total Zn^{2+} binding species of GM-CSF PMφ and BMMφ compared to resting PMφ. Figure 4 shows SEC chromatograms followed by ICPMS analysis representing the total Zn^{2+} binding species of infected and uninfected resting PMφ versus GM-CSF treated PMφ. A higher amount of Zn^{2+} binding species were consistently detected in GM-CSF PMφ compared to that of resting PMφ especially Zn^{2+} species eluting at 27 min..

Effect of GM-CSF is independent of modulation of calprotectin

Calprotectin has been shown to bind Zn^{2+} and possess anti-fungal activity [17]. We asked if GM-CSF altered expression of it. Exposure of cells to GM-CSF did not enhance significantly ($p > 0.05$, t-test) calprotectin expression (Fig. 5).

Discussion

In this study, GM-CSF-activated Mφ restricted intracellular growth of *H. capsulatum* as well as the concentrations of Zn^{2+} and $Fe^{2+/3+}$. Moreover, IL-4 reversed the growth inhibitory properties of activated Mφand increased $[Zn^{2+}]$ in Mφ and yeast cells. Among the metals

analyzed, Zn^{2+} was the most heavily influenced by GM-CSF and IL-4 treatment. These findings prompted us to examine the role of Zn^{2+} in the growth of *H. capsulatum*. Zn^{2+} chelation restricted growth both in medium alone and within Mφ. Furthermore GM-CSF activation was accompanied by changes in the abundance and number of Zn^{2+} binding species. The data provide a link between Zn^{2+} abundance and *H. capsulatum* intracellular survival.

Zn^{2+} is a cofactor for over 300 proteins and required for the survival of most microorganisms [16]. *Salmonella enterica* and *Aspergillus fumigatus* utilize a Zn^{2+} uptake system that is required for Zn^{2+} homeostasis and full virulence [18,19]. Several pathogenic fungi including *Candida al-bicans* and *A. fumigatus* display growth impairment to Zn^{2+} deprivation [20]. Using Zn^{2+} chelators DTPA and TPEN our studies reveal that Zn^{2+} is required for the growth of *H. capsulatum* in medium and can influence intracellular growth. Although our data suggests this chelator also binds Fe^{2+}, a clear advantage exists for the host to restrict both Fe^{2+} and Zn^{2+} during infection with *H. capsulatum*.

Activation of murine Mφ with IFN-γ stimulates the production of NO which is believed to promote degradation of several intracellular pathogens including *H. capsulatum* [21–23]. Indirect and direct evidence also exist for IFN-γ-mediated host restriction of $Fe^{2+/3+}$ availability [3,24–26]. We detected lower levels of $Fe^{2+/3+}$ and Zn^{2+} in IFN-γ and GM-CSF-treated Mφ. GM-CSF is a pleiotropic cytokine that induces myelopoiesis, acts as pro-inflammatory agent, and arms phagocytes to express anti microbial activity [27]. Much of the literature indicates that GM-CSF enhances reactive oxygen intermediates as one mechanism of host defenses. Our data reveal that another antimicrobial defense mechanism is limitation of metals [28,29]. We discovered that Zn^{2+} levels were less in GM-CSF treated Mφ infected with *H. capsulatum* compared to resting infected Mφ.

Host intracellular Zn^{2+} concentrations are controlled by Zn^{2+} importers, exporters, and metal binding proteins such as metallothionens [30]. Zn^{2+} is an essential element required for mammalian cell function, but high concentrations of Zn^{2+} can be toxic therefore regulation of this metal must be tightly controlled [31]. Thus fluctuations in intracellular Zn^{2+} levels must be initiated and/or responded to by the host. Accordingly we detected changes in Zn^{2+} species abundance to accompany GM-CSF induced Zn^{2+} restriction and IL-4 induced Zn^{2+} replenishment. Thus the changes in the number of Zn^{2+} species add further support to the Zn^{2+} level alterations detected. These data also suggest the participation of a host Zn regulatory mechanism influenced by different cytokines during *H. capsulatum* infection.

IL-4 alternatively activates Mφ and thereby inhibits the killing of intracellular and some extracellular organisms *in vitro* [11,32,33]. Overproduction of IL-4 under conditions of altered immunity accelerates *H. capsulatum* infection, but the mechanism remains unclear [10,34, 35]. One mechanism which IL-4 may contribute to organism survival during infection is by reducing NO production [36], but in this study IL-4 reversal of GM-CSF activity was independent of NO production. Another potential mechanism of organism growth enhancement by IL-4 is the alteration of metal homeostasis. IL-4 increases Ca^{2+} movement and accumulation in Mφ [37,38]. Likewise we detected increases in Ca^{2+} levels in *H. capsulatum* isolated from IL-4 exposed Mφ. However, Ca^{2+} chelation had only a minimal effect on intracellular yeast growth, thus suggesting that this metal is not important in the effect of IL-4. Treatment of Mφ with IL-4 has been suggested to make Fe more available to *Mycobacterium tuberculosis* in Mφ [39]. In this study increases in Mφ $Fe^{2+/3+}$ levels were not detected. In contrast, IL-4 treatment partially restored intracellular yeast growth in associating with increasing intracellular Zn^{2+} levels. Thus, Zn^{2+} rather than Fe replenishment following IL-4 treatment of Mφ may contribute to a more permissive environment.

In summary we have shown that cytokine activated Mφ manifest a modulation of metal levels. The data support a crucial role for Zn^{2+} limitation as a key element of host defenses.

Acknowledgments

This work was supported by a Merit Review from the Veterans Affairs and grants AI-73337, and AI-83313 from the National Institute of Allergy and Infectious Diseases

References

1. Wadman M. Poor trial design leaves gene therapy death a mystery. Nat Med 2007;13:1124. [PubMed: 17917642]
2. Howard DH. Intracellular Behavior Of *Histoplasma capsulatum*. J Bacteriol 1964;87:33–8. [PubMed: 14102870]
3. Lane TE, Wu-Hsieh BA, Howard DH. Iron limitation and the gamma interferon-mediated antihistoplasma state of murine macrophages. Infect Immun 1991;59:2274–8. [PubMed: 1904840]
4. Newman SL, Gootee L. Colony-stimulating factors activate human macrophages to inhibit intracellular growth of *Histoplasma capsulatum* yeasts. Infect Immun 1992;60:4593–7. [PubMed: 1398972]
5. Allendoerfer R, Deepe GS Jr. Intrapulmonary response to *Histoplasma capsulatum* in gamma interferon knockout mice. Infect Immun 1997;65:2564–9. [PubMed: 9199420]
6. Huang CC, Yang MH, Shih TS. Automated on-line sample pretreatment system for the determination of trace metals in biological samples by inductively coupled plasma mass spectrometry. Anal Chem 1997;69:3930–9. [PubMed: 9322431]
7. Sarmiento-Gonzalez A, Marchante-Gayon JM, Tejerina-Lobo JM, Paz-Jimenez J, Sanz-Medel A. High-resolution ICP-MS determination of Ti, V, Cr, Co, Ni, and Mo in human blood and urine of patients implanted with a hip or knee prosthesis. Anal Bioanal Chem 2008;391:2583–9. [PubMed: 18537030]
8. Deepe GS Jr, Gibbons RS, Smulian AG. *Histoplasma capsulatum* manifests preferential invasion of phagocytic subpopulations in murine lungs. J Leukoc Biol 2008;84:669–78. [PubMed: 18577715]
9. Deepe GS Jr, Gibbons R. Recombinant murine granulocyte-macrophage colony-stimulating factor modulates the course of pulmonary histoplasmosis in immunocompetent and immunodeficient mice. Antimicrob Agents Chemother 2000;44:3328–36. [PubMed: 11083636]
10. Szymczak WA, Deepe GS Jr. The CCL7-CCL2-CCR2 axis regulates IL-4 production in lungs and fungal immunity. J Immunol 2009;183:1964–74. [PubMed: 19587014]
11. Vouldoukis I, Becherel PA, Riveros-Moreno V, et al. Interleukin-10 and interleukin-4 inhibit intracellular killing of *Leishmania infantum* and *Leishmania major* by human macrophages by decreasing nitric oxide generation. Eur J Immunol 1997;27:860–5. [PubMed: 9130636]
12. Loke P, Nair MG, Parkinson J, Guiliano D, Blaxter M, Allen JE. IL-4 dependent alternatively-activated macrophages have a distinctive in vivo gene expression phenotype. BMC Immunol 2002;3:7. [PubMed: 12098359]
13. Canzoniero LM, Sensi SL, Choi DW. Measurement of intracellular free zinc in living neurons. Neurobiol Dis 1997;4:275–9. [PubMed: 9361304]
14. Outten CE, O'Halloran TV. Femtomolar sensitivity of metalloregulatory proteins controlling zinc homeostasis. Science 2001;292:2488–92. [PubMed: 11397910]
15. O'Sullivan WJ, Smithers GW. Stability constants for biologically important metal-ligand complexes. Methods Enzymol 1979;63:294–336. [PubMed: 41156]
16. Rink L, Haase H. Zinc homeostasis and immunity. Trends Immunol 2007;28:1–4. [PubMed: 17126599]
17. Urban CF, Ermert D, Schmid M, et al. Neutrophil extracellular traps contain calprotectin, a cytosolic protein complex involved in host defense against Candida albicans. PLoS Pathog 2009;5:e1000639. [PubMed: 19876394]
18. Ammendola S, Pasquali P, Pistoia C, et al. High-affinity Zn2+ uptake system ZnuABC is required for bacterial zinc homeostasis in intracellular environments and contributes to the virulence of *Salmonella enterica*. Infect Immun 2007;75:5867–76. [PubMed: 17923515]

19. Moreno MA, Ibrahim-Granet O, Vicentefranqueira R, et al. The regulation of zinc homeostasis by the ZafA transcriptional activator is essential for *Aspergillus fumigatus* virulence. Mol Microbiol 2007;64:1182–97. [PubMed: 17542914]
20. Lulloff SJ, Hahn BL, Sohnle PG. Fungal susceptibility to zinc deprivation. J Lab Clin Med 2004;144:208–14. [PubMed: 15514589]
21. Lane TE, Otero GC, Wu-Hsieh BA, Howard DH. Expression of inducible nitric oxide synthase by stimulated macrophages correlates with their antihistoplasma activity. Infect Immun 1994;62:1478–9. [PubMed: 7510670]
22. Nakamura LT, Wu-Hsieh BA, Howard DH. Recombinant murine gamma interferon stimulates macrophages of the RAW cell line to inhibit intracellular growth of *Histoplasma capsulatum.* Infect Immun 1994;62:680–4. [PubMed: 8300224]
23. Kagaya K, Watanabe K, Fukazawa Y. Capacity of recombinant gamma interferon to activate macrophages for Salmonella-killing activity. Infect Immun 1989;57:609–15. [PubMed: 2492266]
24. Byrd TF, Horwitz MA. Interferon gamma-activated human monocytes downregulate transferrin receptors and inhibit the intracellular multiplication of *Legionella pneumophila* by limiting the availability of iron. J Clin Invest 1989;83:1457–65. [PubMed: 2496141]
25. Nairz M, Fritsche G, Brunner P, Talasz H, Hantke K, Weiss G. Interferon-gamma limits the availability of iron for intramacrophage *Salmonella typhimurium.* Eur J Immunol 2008;38:1923–36. [PubMed: 18581323]
26. Wagner D, Maser J, Moric I, et al. Changes of the phagosomal elemental concentrations by *Mycobacterium tuberculosis* Mramp. Microbiology 2005;151:323–32. [PubMed: 15632449]
27. Hamilton JA. Colony-stimulating factors in inflammation and autoimmunity. Nat Rev Immunol 2008;8:533–44. [PubMed: 18551128]
28. Denis M, Ghadirian E. Granulocyte-macrophage colony-stimulating factor restricts growth of tubercle bacilli in human macrophages. Immunol Lett 1990;24:203–6. [PubMed: 2116996]
29. Ding AH, Nathan CF, Stuehr DJ. Release of reactive nitrogen intermediates and reactive oxygen intermediates from mouse peritoneal macrophages. Comparison of activating cytokines and evidence for independent production. J Immunol 1988;141:2407–12. [PubMed: 3139757]
30. Murakami M, Hirano T. Intracellular zinc homeostasis and zinc signaling. Cancer Sci 2008;99:1515–22. [PubMed: 18754861]
31. Sugarman B. Zinc and infection. Rev Infect Dis 1983;5:137–47. [PubMed: 6338570]
32. Cenci E, Romani L, Mencacci A, et al. Interleukin-4 and interleukin-10 inhibit nitric oxide-dependent macrophage killing of *Candida albicans*. Eur J Immunol 1993;23:1034–8. [PubMed: 8477799]
33. Denis M, Gregg EO, Ghandirian E. Cytokine modulation of *Mycobacterium tuberculosis* growth in human macrophages. Int J Immunopharmacol 1990;12:721–7. [PubMed: 2127260]
34. Allen HL, Deepe GS Jr. Apoptosis modulates protective immunity to the pathogenic fungus *Histoplasma capsulatum*. J Clin Invest 2005;115:2875–85. [PubMed: 16151533]
35. Gildea LA, Gibbons R, Finkelman FD, Deepe GS Jr. Overexpression of interleukin-4 in lungs of mice impairs elimination of *Histoplasma capsulatum*. Infect Immun 2003;71:3787–93. [PubMed: 12819061]
36. Rutschman R, Lang R, Hesse M, Ihle JN, Wynn TA, Murray PJ. Cutting edge: Stat6-dependent substrate depletion regulates nitric oxide production. J Immunol 2001;166:2173–7. [PubMed: 11160269]
37. Sharma P, Chakraborty R, Wang L, et al. Redox regulation of interleukin-4 signaling. Immunity 2008;29:551–64. [PubMed: 18957266]
38. Albuquerque PC, Nakayasu ES, Rodrigues ML, et al. Vesicular transport in *Histoplasma capsulatum*: an effective mechanism for trans-cell wall transfer of proteins and lipids in ascomycetes. Cell Microbiol 2008;10:1695–710. [PubMed: 18419773]
39. Kahnert A, Seiler P, Stein M, et al. Alternative activation deprives macrophages of a coordinated defense program to *Mycobacterium tuberculosis*. Eur J Immunol 2006;36:631–47. [PubMed: 16479545]

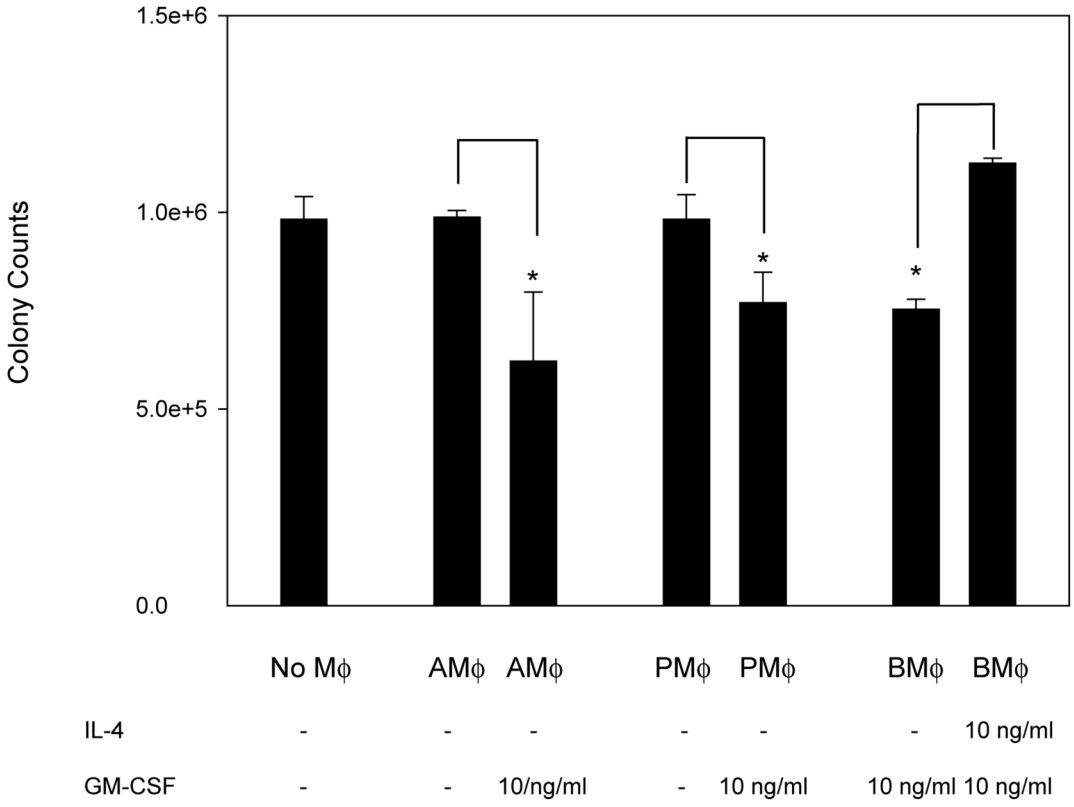

Figure 1.

GM-CSF activates Mφ to exert antifungal activity and IL-4 inhibits activation. Colony counts from *H. capsulatum* in culture alone, resting AMφ, GM-CSF treated AMφ, resting PMφ, GM-CSF treated PMφ, and GM-CSF BMMφ pretreated with IL-4 for 24hr. Data represent mean ± SEM from 3 experiments. * P< .05 (student's *t* test) compared to resting PMφ.

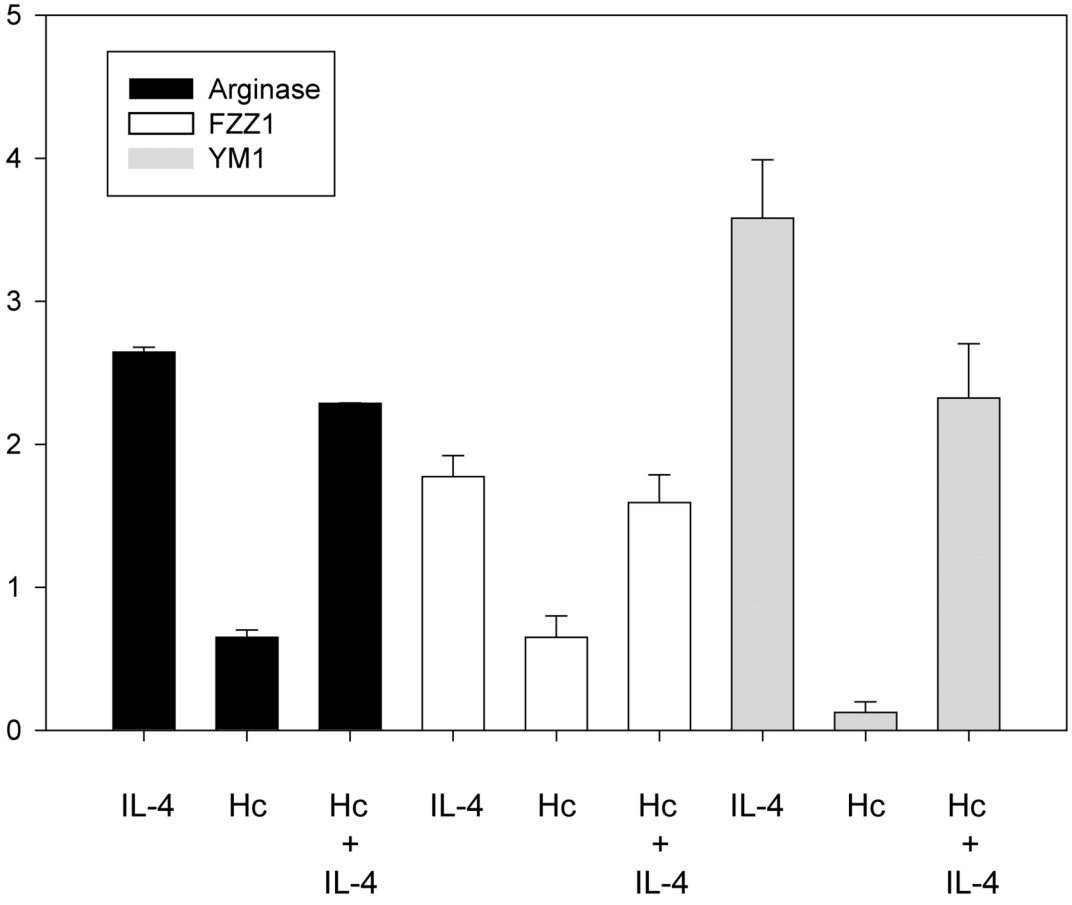

Figure 2.
Expression of IL-4-regulated genes in BMMφ. qRT-PCR of arginase, FIZZ1, and YM1 expression in BMMφ pretreated with 10 ng of IL-4 for 24hr, infected with *H. capsulatum* (without IL-4), or IL-4 treated and infected. Expression levels were normalized to uninfected BMMφ without IL-4. Data represent mean ± SEM from 3 experiments.

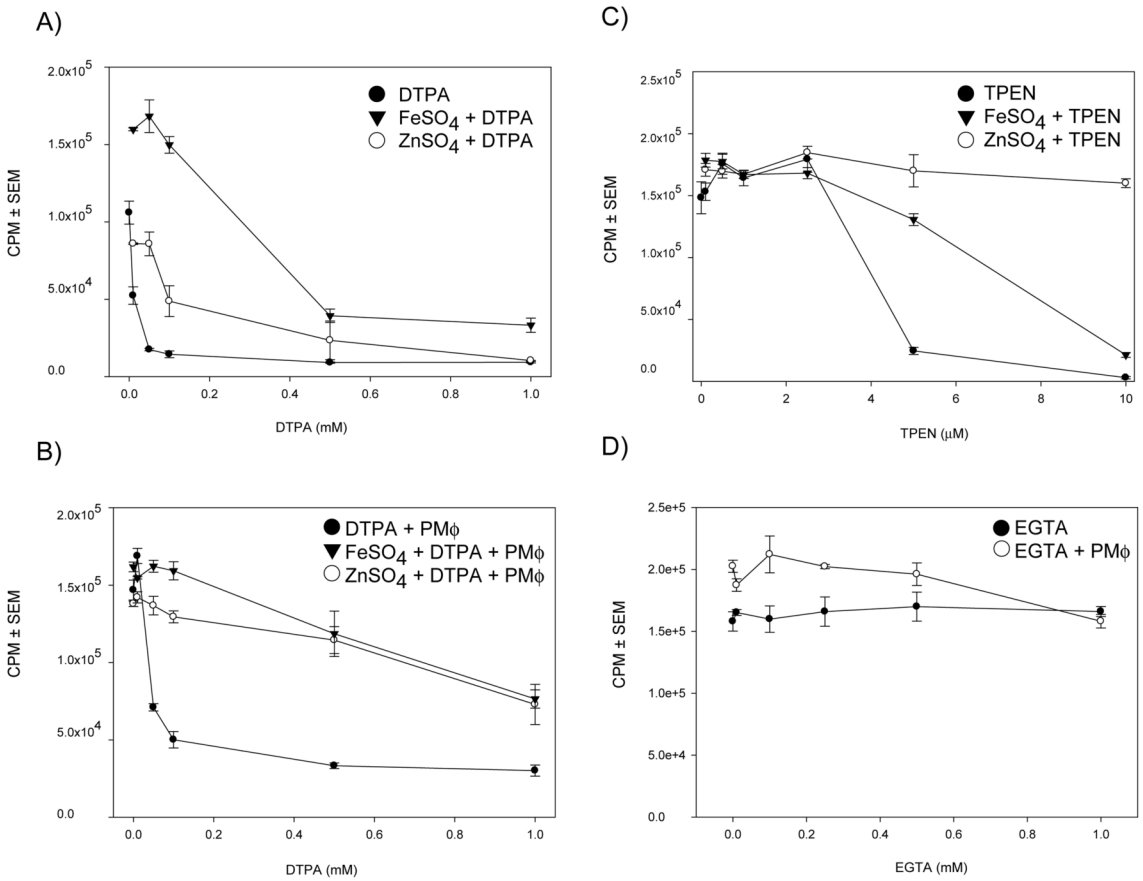

Figure 3.

Zn chelation inhibits *H. capsulatum* growth. CPM from tritiated leucine assays of *H. capsulatum* in A) media containing DTPA (filled circle), in the presence of DTPA + $FeSO_4$ (filled triangle), or TPEN + $ZnSO_4$ (unfilled circle) B.) PMφ. C.) media containing TPEN (filled circle), in the presence of TPEN + $FeSO_4$ (filled triangle), or TPEN + $ZnSO_4$ (unfilled circle) D) media containing EGTA (filled circle) and media containing EGTA + PMφ (unfilled circle). Data represent the mean ± SEM of triplicates from 1 representative experiment of 3.

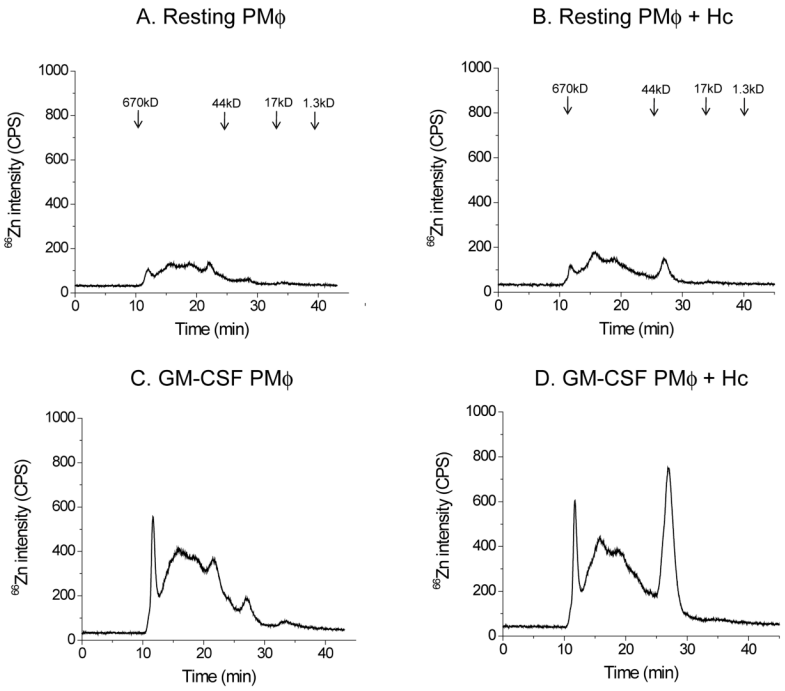

Figure 4.

Mφ activation and *H. capsulatum* infection regulate host Zn binding species. Size exclusion chromatography followed by ICPMS analysis of Zn species in A.) resting PMφ B.) resting PMφ infected with *H. capsulatum* C.) GM-CSF treated PMφ D) infected GM-CSF treated PMφ. Yeasts were removed before SEC and ICPMS analysis. Molecular weight standards are listed above A and B.

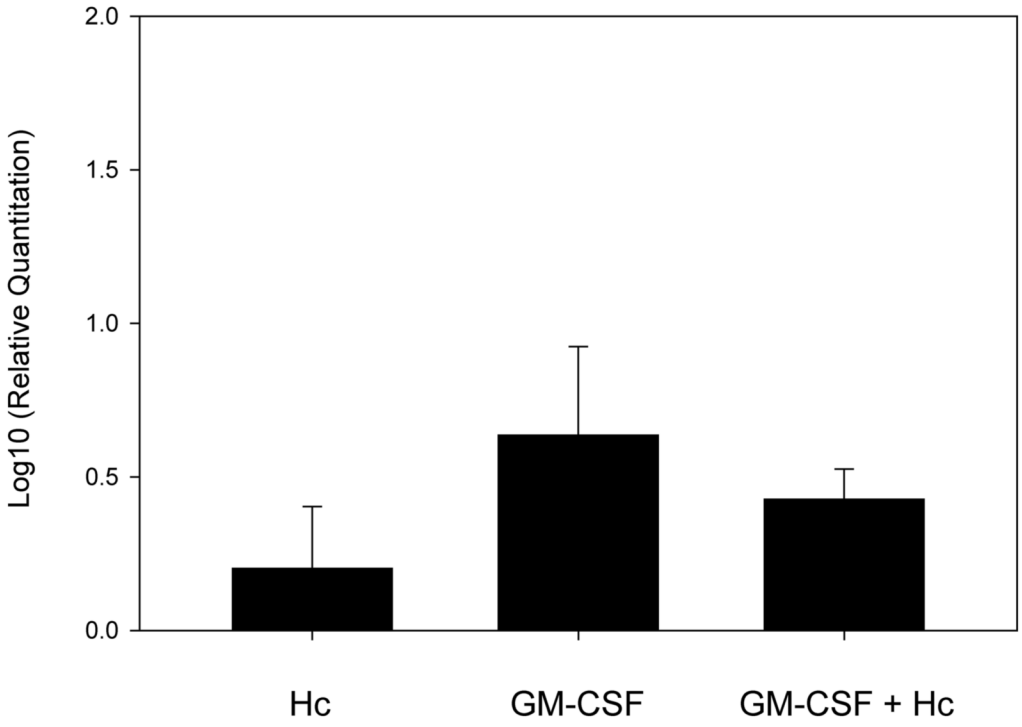

Figure 5.
GM-CSF does not increase calprotectin expression in PMφ. qRT-PCR of calprotectin expression of *H. capsulatum* infected resting PMφ, uninfected PMφ pretreated with 10 ng of GM-CSF for 24hr, no infection or GM-CSF infected PMφ. Expression levels were normalized to un-infected PMφ without GM-CSF treatment. Data represent mean ± SEM from 3 experiments. Hc = *H. capsulatum.*

Table 1

Operating conditions for HPLC-ICPMS

ICPMS parameters	
Forward power (W)	1500
Plasma gas flow rate (L min^{-1})	15.0
Carrier gas flow rate (L min^{-1})	1.01
Isotopes monitored for SEC	^{66}Zn
Isotopes monitored for flow injection	^{23}Na, ^{24}Mg, ^{39}K, ^{44}Ca, ^{55}Mn, ^{57}Fe, ^{60}Ni, ^{63}Cu, ^{66}Zn
Collision gas (mL H_2 min^{-1})	3.2
Quadrupole bias (V)	−16
Octopole bias (V)	−18
SEC chromatographic parameters	
Column	Superdex 200 10/300 GL
Mobile phase	30 mM Tris-HCl buffer, pH 7.5
Flow rate (mL min^{-1})	0.7
Injection volume (μL)	100
Flow injection parameters	
Column	N/A
Mobile phase	0.1 % nitric acid
Flow rate (mL min^{-1})	0.8
Injection volume (μL)	50

Table 2

Metal Levels

Metal levels from 1×10^5 uninfected and *H. capsulatum*-infected Mφ cells								
	Resting PMφ		GM-CSF PMφ		GM-CSF BMMφ		GM-CSF BMMφ + IL-4	
	AVG	RSD	AVG	RSD	AVG	RSD	AVG	RSD
Mg	2240	2%	790	2%	1210	3%	1270	2%
Ca	3700	3%	1750	5%	2220	5%	2044	2%
Fe	1360	2%	664[a]	5%	932	3%	1002	5%
Zn	190	6%	89	6%	179	5%	153	2%
Cu	57	5%	23	6%	22	3%	20	1%
Mn	8	9%	<1	3%	<1	4%	<1	2%

	Resting PMφ + Hc		GM-CSF PMφ + Hc		GM-CSF BMMφ +Hc		GM-CSF BMMφ + IL-4 + Hc	
	AVG	RSD	AVG	RSD	AVG	RSD	AVG	RSD
Mg	778	2%	954	2%	1300	1%	1310	3%
Ca	1780	8%	1350	4%	2110	1%	2032	2%
Fe	680	6%	275[a]	7%	566	3%	597	7%
Zn	131	8%	28[a]	6%	63[a]	2%	162[b]	10%
Cu	24	11%	22	2%	26	3%	24	8%
Mn	<1	9%	<1	12%	<1	2%	<1	1%

H. capsulatum metal levels from 1×10^7 cells following isolation from infected Mφ and culture alone.										
	Resting PMφ		GM-CSF PMφ		GM-CSF BMMφ		GM-CSF BMMφ + IL-4		Culture Alone	
	AVG	RSD	AVG	RSD	AVG	RSD	AVG	RSD	AVG	RSD
K	25500	1%	14000	1%	13400	1%	28200	2%	13400	1%
Mg	17000	1%	3400	9%	2400	8%	4100	12%	1800	9%
Ca	38300	1%	11800[a]	7%	5600[a]	12%	12500[b]	10%	4400	15%
Fe	6400	4%	4300	3%	1700[a]	5%	2160	7%	4650	2%
Zn	1900	1%	1200[a]	2%	500[a]	1%	1100[b]	1%	600	1%
Cu	406	2%	219	2%	73	6%	50	25%	46	3%
Mn	42	16%	53	15%	21	26%	55	2%	36	15%

H. capsulatum **metal levels from 1×10^7 cells following isolation from infected Mφ and culture alone.**

	Resting PMφ		GM-CSF PMφ		GM-CSF BMMφ		GM-CSF BMMφ + IL-4		Culture Alone	
	AVG	**RSD**	**AVG**	**RSD**	**AVG**	**RSD**	**AVG**	**RSD**	**AVG**	**RSD**
Ni	175	9%	147	15%	59	23%	102	7%	56	19%

NOTE: Data are a mean of 3 experimental replicates represented in parts per billion (ppb) (1 ppb=1 μg L^{-1}). RSD, Relative standard deviation, Hc, Histoplasma capsulatum, PMφ, peritoneal macrophages, BMMφ, bone marrow derived macrophages.

[a] P<.05 (ANOVA analysis) compared to resting infected (Hc) PMφ, and

[b] compared to infected (Hc) GM-CSF BMMφ